Electron impact ionization of neon and neonic ions under distorted-wave Born approximation*

Zhou Li-Xia(周丽霞)† and Yan You-Guo(燕友果)

College of Science, China University of Petroleum, Qingdao 266580, *China*

(Received 28 June 2013; revised manuscript received 23 October 2013; published online 1 April 2014)

The (e, 2e) triple differential cross sections of 2s orbitals of neon and neonic ions ($Z = 11$–14) are calculated using a distorted-wave Born approximation under coplanar asymmetric geometry. The calculated results show that, with the increase in the nuclear charge number Z, the amplitude of triple differential cross sections decreases. The angle difference between the binary peak position and the direction of momentum transfer gradually increases with the increase in the nuclear charge Z, and a new structure appears at an ejected angle $90° < \theta_2 < 120°$. Three kinds of collision processes are proposed to illustrate the formation mechanism of such collision peaks.

Keywords: (e, 2e) reaction, distorted-wave Born approximation, triple differential cross sections

PACS: 34.80.Dp, 34.50.Fa **DOI:** 10.1088/1674-1056/23/5/053402

1. Introduction

Electron impact ionization of atomic, molecular, and ionic targets is a useful tool to study the target particle structure and ionization process of interaction, commonly known as the (e, 2e) reaction. Over the past few decades, a large number of experimental and theoretical studies of (e, 2e) triple differential cross sections (TDCS's) for atoms have been performed, which has provided abundant information about (e, 2e) dynamics.[1–3]

However, due to the low density of the ion source, the experimental research of TDCS's of ions has never been reported. The first theoretical study was conducted by Roy *et al.*,[4] where they calculated the (e, 2e) TDCS's of He^+ using the Coulomb–Born approximation with an incident energy range of 200–3000 eV under symmetric geometry. Biswas *et al.*[5,6] calculated the (e, 2e) TDCS's of He^+ and Li^+ under coplanar asymmetric geometry, adopting Eikonal approximation including post-collision interaction. They found that the intensity of the recoil peak would increase at lower incident energy. Shi *et al.*[7] calculated the TDCS's of hydrogenic ions with nuclear charge $Z = 2$–5 at an incident energy of 1000 eV. They found one forward peak at $Z = 4$, and ascribed it to a double-binary collision. Khajuria1 *et al.*[8] studied the TDCS's of $Li^+(1s^2)$, $Rb^+(4p^6)$, $Cs^+(5p^6)$, $Cu^+(3d^{10})$, and $Ag^+(4d^{10})$ ions in the coplanar to perpendicular plane geometry using distorted-wave Born approximation (DWBA), and the effect of the post-collision interaction was discussed. They found an interference dip in the cross section for each target. In our previous study, the TDCS's of Cu^+ (3p) under coplanar asymmetric geometry and Ag^+ (4p, 4s) under coplanar symmetric geometry were discussed,[9,10] and the binary peaks of Cu^+ (3p) and Ag^+ (4p) showed abnormal splits.

In this paper, we calculate the (e, 2e) TDCS's of Ne and neonic ions ($Z = 11$–14) under coplanar asymmetric geometry using the DWBA theory. The incident electron energy is 1000 eV, the ejected electron energy is 61 eV, and the scattering electron angles are set at 4°, 7°, and 10°, respectively. The amplitude and peak position of binary and recoil peaks are studied, and some kinds of double-binary collision and triple-binary collision are discussed in detail.

2. Theory

Considering an atom or ion target ionized by an incident electron with momentum k_0 followed by two outgoing electrons with momenta k_1 and k_2, the TDCS for such a process could be described by the DWBA theory as follows:[11]

$$\frac{\mathrm{d}^3\sigma^{\mathrm{DWBA}}}{\mathrm{d}\Omega_1\,\mathrm{d}\Omega_2\,\mathrm{d}E_1} = (2\pi)^4\frac{k_1k_2}{k_0}\sum_{\mathrm{av}}[|f|^2+|g|^2-\mathrm{Re}(f^*g)], \quad (1)$$

$$f = \left\langle \chi^{(-)}(k_1,r_1)\chi^{(-)}(k_2,r_2)\left|\frac{1}{r_{12}}\right|\chi^{(+)}(k_0,r_0)\psi_{nl}\right\rangle, \quad (2)$$

$$g = \left\langle \chi^{(-)}(k_1,r_2)\chi^{(-)}(k_2,r_1)\left|\frac{1}{r_{12}}\right|\chi^{(+)}(k_0,r_0)\psi_{nl}\right\rangle. \quad (3)$$

Here, $\sum_{\mathrm{av}}$ represents the sum over the final and the average over the initial magnetic and spin degeneracy, ψ_{nl} is the orbital of the ion target, $\chi^{(+)}$ denotes the distorted wave of the incident electron generated in the equivalent local ground-state potential V_{D} of the ion target, and $\chi^{(-)}$ is the distorted wave of outgoing electrons generated in the equivalent local ground-state potential of an ion in the final channels. The $\chi^{(+)}$ and $\chi^{(-)}$ are both orthogonal to ψ_{nl}. The equivalent local ground-state

*Project supported by the Fundamental Research Funds for the Central University of China (Grant No. 13CX02019A).

†Corresponding author. E-mail: zhoulx@upc.edu.cn

© 2014 Chinese Physical Society and IOP Publishing Ltd

potential $V_{\rm D}$, i.e., distorting potential, is the sum of direct potential $V_{\rm D}$ and exchange potential $V_{\rm E}$. The direct potential $V_{\rm D}$ is obtained by integrating the target ion radial orbital $u_{nl}(r)$[11]

$$V_{\rm D}(r) = \sum_{nl} N_{nl} \int {\rm d}r' [u_{nl}(r')]^2 / r_>, \tag{4}$$

where $r_>$ is the greater one among r and r', N_{nl} is the number of electrons in orbital ψ_{nl}. The spin average static exchange potential $V_{\rm E}$ is given by[12]

$$V_{\rm E}(r) = 0.5\left\{E - V_{\rm D}(r) + \frac{3}{10}[3\pi^2\rho(r)]^{2/3}\right\} - 0.5\left\{[E - V_{\rm D}(r) + \frac{3}{10}[3\pi^2\rho(r)]^{2/3}]^2 + 4\pi\rho(r)\right\}^{1/2}, \tag{5}$$

where $\rho(r)$ is the electron density. The equivalent distorting potential $V_{00}(r) = V_{\rm D}(r) + V_{\rm E}(r)$ is described as

$$V_{00}(r) = V_{\rm D}(r) + V_{\rm E}(r). \tag{6}$$

3. Results and discussion

Figure 1 shows the (e, 2e) TDCS's of Ne and neonic ions under coplanar asymmetric geometry within the DWBA theory. The incident electron energy is 1000 eV, and the ejected electron energy is 61 eV. Figures 1(a)–1(c) represent the TDCS's at a scattering electron angle of $\theta_1 = 4^\circ$, 7°, and 10°, respectively.

From Fig. 1, it can be seen that the amplitude of TDCS's decrease gradually with the increase in the nuclear charge Z. Two obvious peaks appear at about 60° and 240°, which are well known as binary and recoil peaks.[7,8] The orbital electrons are knocked out by incident electrons, forming the binary peak, which always appears in the direction of momentum transfer $\boldsymbol{K}$. If the ejected electrons are recoiled by the target ion, the recoil peak will emerge. The recoil peak always appears in the opposite direction of momentum transfer $\boldsymbol{K}$.

Table 1 gives the peak position of binary peak ($\theta_{\rm peak}$) and the direction of momentum transfer $\theta_{\rm K}$. From Table 1, it can be seen that the position of binary peak $\theta_{\rm peak}$ of Ne just accords well with the angle $\theta_{\rm K}$ of the momentum transfer direction. However, with the increase in the nuclear charge Z, the difference between them gradually enlarges, and $\theta_{\rm peak}$ shifts to a higher angle than $\theta_{\rm K}$. For Al^{3+} and Si^{4+}, with scattering electron angle $\theta_1 = 10^\circ$, the difference between them reaches 11° and 13°, respectively. Such a great difference indicates that the (e, 2e) reaction process for ions is more complex than that of atoms. In the reaction, one kind of double-binary collision[7] may occur, as shown in Fig. 2: the incident electron is first scattered elastically by the nucleus, and the incident electron will deflect with an angle θ. Then, the incident electron will collide with the orbital electron. Subsequently, the incident electron emerges at angle θ_1, and the orbital electron will be ejected with an angle of θ_2. When the nuclear number Z of the target ion increases gradually, the scattering angle θ will increase, which induces the ejected electron e_2 to emerge in the higher angle θ_2.

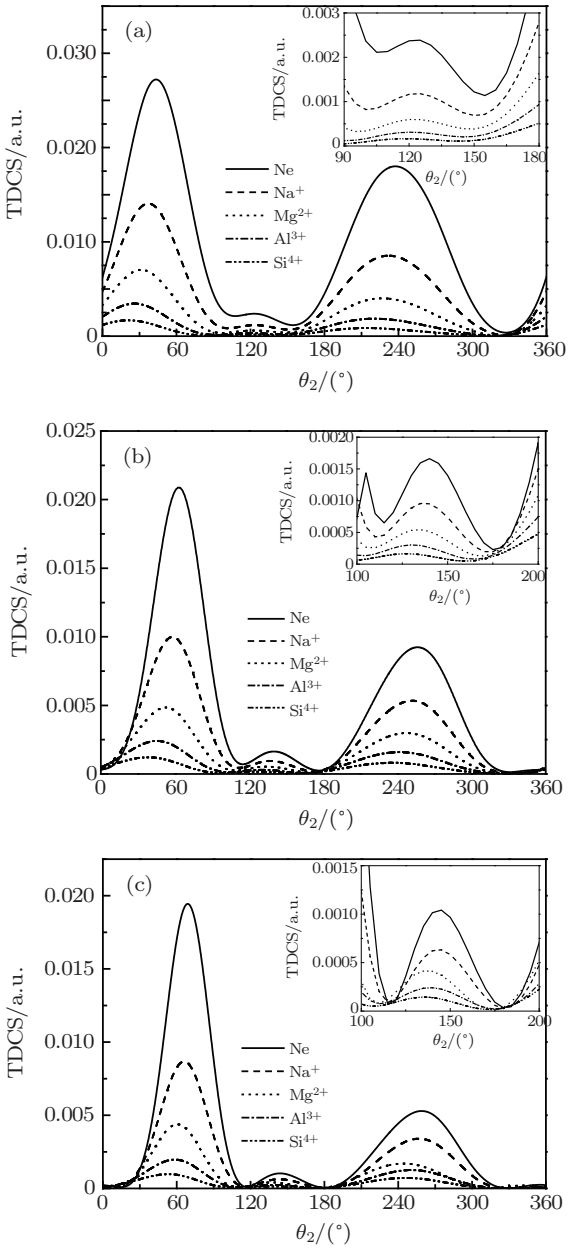


Fig. 1. (e, 2e) TDCS's of electron impact ionization of 2s orbitals of Ne and neonic ions with incident energy $E_0 = 1000$ eV and ejected electron energy $E_2 = 61$ eV under coplanar asymmetric geometry: (a) scattering electron angle $\theta_1 = 4^\circ$, (b) scattering electron angle $\theta_1 = 7^\circ$, and (c) scattering electron angle $\theta_1 = 10^\circ$.

In order to confirm the dynamic process shown in Fig. 2, a simulated (e, 2e) reaction triple differential cross section is conducted. The probability of an (e, 2e) reaction is related to two factors. The first is the probability of elastic scattering. The second is the electron density that the scattered incident electron goes through. High density commonly means high collision probability. As a result, the probability of (e, 2e) reaction is determined by the product of these two terms.

Table 1. Direction of momentum transfer θ_K and the position of binary peak θ_{peak} for Ne and neonic ions with different scattering angle θ_1.

Target	θ_1/(°)	θ_K/(°)	θ_{peak}/(°)
Ne	4	48	45
	7	61	65
	10	67	70
Na^+	4	40	35
	7	54	60
	10	61	65
Mg^{2+}	4	33	30
	7	47	50
	10	55	60
Al^{3+}	4	26	25
	7	40	45
	10	49	60
Si^{4+}	4	21	20
	7	33	40
	10	42	55

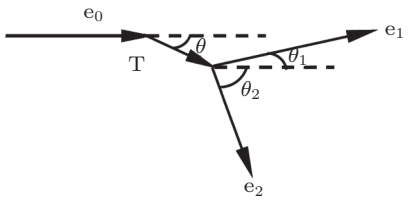


Fig. 2. Sketch of one kind of double-binary collision process for an ionic target. T denotes the target nucleus.

The probability of elastic scattering can be estimated by the following Rutherford scattering cross section:[13]

$$\theta = 2\cot^{-1}\left(4\pi\varepsilon_0 \frac{2E_0}{Ze^2} b\right), \tag{7}$$

$$\frac{\mathrm{d}\sigma}{\mathrm{d}\theta} = \left(\frac{1}{4\pi\varepsilon_0}\right)^2 \pi \left(\frac{Ze^2}{2E_0}\right)^2 \frac{\cos(\theta/2)}{\sin^3(\theta/2)}, \tag{8}$$

where Z is the effective nuclear charge, and b is the impact parameter.

Here, Al^{3+} is selected as the research object, and Z is 2.48.[14] Figure 3 shows the normalized Rutherford scattering cross section, normalized electron density distribution, and normalized product of these two terms. For the product above 90%, we can have impact parameter $b \geq 0.7$ a.u., and the corresponding scattering angle $\theta \leq 5.5°$.

Considering the symmetry, the range of θ is chosen to be $\pm 5.5°$, $\pm 4.5°$, $\pm 3.5°$, $\pm 2.5°$, $\pm 1.5°$ and $0°$, respectively. As we have considered the electron elastically scattering of ion in the first collision, we adopt the distorting potential of Ne(2s) instead of that of Al^{3+}(2s) to obtain the distorted wave function $\chi^{(+)}$ in the second collision.[13] The TDCS's of the second collision have been calculated and the scattering angles are set as $\theta_1 \pm 5.5°, \theta_1 \pm 4.5°$, $\theta_1 \pm 3.5°$, $\theta_1 \pm 2.5°$, $\theta_1 \pm 1.5°$, and θ_1, respectively. Then we weight sum over these calculated TDCS's to simulate the TDCS of Al^{3+}(2s) with scattering angle θ_1.

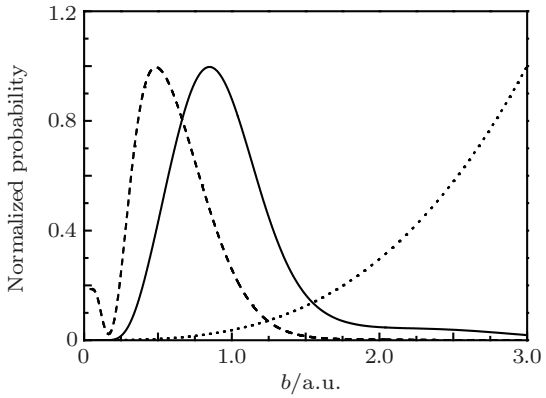


Fig. 3. Dotted line presents the normalized probability of elastic scattering for Al^{3+}. Dashed line presents the normalized radial electron density distribution for Al^{3+}(2s). The solid line presents the normalized product of the probability of elastic scattering and the radial density distribution for Al^{3+}(2s).

In contrast, the normalized simulation result for Al^{3+}(2s) at $\theta_1 = 10°$ and the normalized DWBA TDCS are shown in Fig. 4(a). It can be seen that the position of binary peaks of two lines both appear at 60°, which confirms the validity of our proposed binary collision process, as shown in Fig. 2.

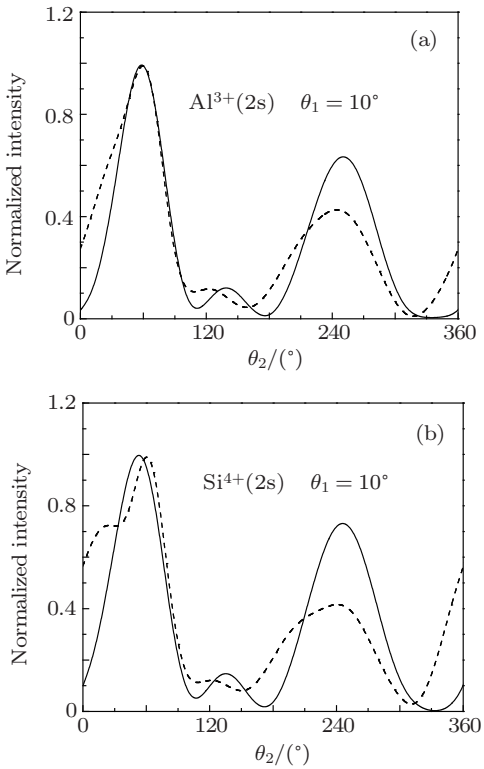


Fig. 4. Normalized TDCS's of DWBA and simulated calculation. Solid lines denote the normalized DWBA TDCS's calculated with an incident energy of 1000 eV and an ejected energy of 61 eV at $\theta_1 = 10°$ under coplanar asymmetric geometry. Dashed lines present the normalized simulated TDCS's: (a) Al^{3+}(2s) and (b) Si^{4+}(2s).

The normalized DWBA calculation and the normalized simulated TDCS of Si^{4+}(2s) at $\theta_1 = 10°$ are also given in Fig. 4(b), and their binary peaks are positioned at 55° and 60.5°, respectively. The difference between them is largely smaller than that of the DWBA TDCS θ_{peak} and the direction

of momentum transfer $\theta_{K,}$ as shown in Table 1. This result also validates the rationality of our proposed binary collision process.

In Figs. 1(a)–1(c), one new peak emerges in the range of $90^\circ < \theta_2 < 120^\circ$. With the increase in the nuclear charge Z, the amplitude of TDCS's decreases and this new structure almost disappears for Al^{3+} and Si^{4+}. This new structure may originate from one kind of double-binary collision or triple-binary collision process as shown in Figs. 5(a) and 5(b). In Fig. 5(a), the incident electron collides with the orbital electron and knocks it out. Then, the ejected orbital electron elastically collides with the nucleus, and emerges in the region of $\theta_2 > 90^\circ$. In Fig. 5(b), the incident electron is scattered elastically by the nucleus firstly and then collides with the orbital electron and knocks it out. The ejected orbital electron is scattered elastically by the nucleus again and emits in the angle $\theta_2 > 90^\circ$. For the above two processes, they have certain probability to coexist in the same (e, 2e) reaction.

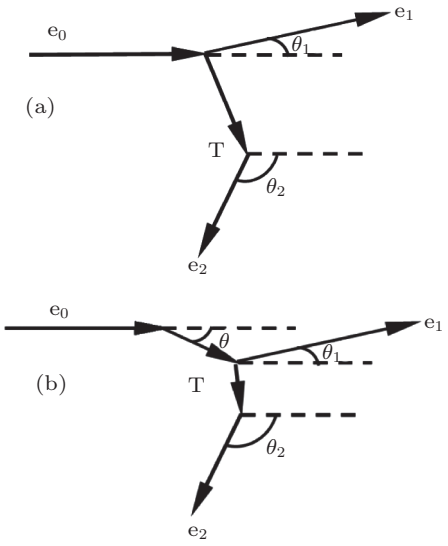


Fig. 5. Sketch of collision processes for the peak in the range of $90^\circ < \theta_2 < 120^\circ$. (a) Another kind of double-binary collision process for an ionic target. (b) One kind of triple-binary collision processes. The T denotes the target nucleus.

4. Conclusions

We have calculated the (e, 2e) TDCS's of 2s orbitals of a neon atom and neonic ions ($Z = 11$–14) using the distorted-wave Born approximation under coplanar asymmetric geometry. The incident electron energy is 1000 eV, the ejected electron energy is 61 eV, and the scattering electron angles are set at 4°, 7°, and 10°. The calculated results show that, with the increase in the nuclear charge number Z, the amplitude of TDCS's decreases. For a 2s orbital of Ne, the binary peak position appears in the momentum transfer direction. While with the increase in Z, the angle difference between the binary peak position and the angle of momentum transfer increases gradually. For Al^{3+} and Si^{4+}, the difference between them reaches 11° and 13°, respectively. It is considered that one kind of double-binary collision occurs in an (e, 2e) reaction. In addition, some new structures appear in the region of $90^\circ < \theta_2 < 120^\circ$. Such new structures may be ascribed to another kind of double-binary collision or one kind of triple-binary collision process.

References

[1] Staicu Casagrande E M, Naja A, Mezdari F, Lahmam-Bennani A, Bolognesi P, Joulakian B, Chuluunbaatar O, Al-Hagan O, Madison D H, Fursa D V and Bray I 2008 *J. Phys. B* **41** 025204
[2] Ren X, Senftleben A, Pflüger T, Holzwarth M, Dorn A, Bartschat K, Bray I, Fursa D V, Colgan J, Pindzola M S, Al-Hagan O, Madison D H and Ullrich J 2010 *J. Phys.: Conf. Ser.* **212** 012003
[3] Ren X, Pfluger T, Xu S, Colgan J, Pindzola M S, Senftleben A, Ullrich J and Dorn A 2012 *Phys. Rev. Lett.* **109** 123202
[4] Roy A, Roy K and Sil N C 1982 *J. Phys. B* **15** 1289
[5] Biswas R and Sinha C 1995 *J. Phys. B* **28** 1311
[6] Biswas R and Sinha C 1994 *Phys. Rev. A* **50** 354
[7] Shi Q C, Chen Z J, Chen J and Xu K Z 1997 *J. Phys. B* **30** 2859
[8] Khajuria Y and Tripathi D N 1999 *Phys. Rev. A* **59** 1197
[9] Zhou L X and Yan Y G 2010 *Chin. Phys. B* **19** 073401
[10] Zhou L X and Yan Y G 2012 *Chin. Phys. B* **21** 093401
[11] McCarthy I E 1995 *Aust. J. Phys.* **48** 1
[12] Gianturco F A and Scialla S 1987 *J. Phys. B* **20** 3171
[13] Chen L Q, Chen X J, Wu X J, Shan X and Xu K Z 2005 *J. Phys. B* **38** 1371
[14] Chen L M, Kang T R and Cheng Z J 2006 *J. China West Normal University* **27** 271 (in Chinese)